IOPscience iopscience.iop.org

Home Search Collections Journals About Contact us My IOPscience

The dielectric spectroscopy of human red blood cells: the differentiation of old from fresh cells

This content has been downloaded from IOPscience. Please scroll down to see the full text.

2017 Physiol. Meas. 38 1335

(http://iopscience.iop.org/0967-3334/38/7/1335)

View the table of contents for this issue, or go to the journal homepage for more

Download details:

IP Address: 132.64.28.69
This content was downloaded on 02/08/2017 at 12:40

Please note that terms and conditions apply.

You may also be interested in:

Dielectric response of biconcave erythrocyte membranes to glucose
L Livshits, A Caduff, M S Talary et al.

Dielectric inspection of erythrocyte morphology
Yoshihito Hayashi, Ikuya Oshige, Yoichi Katsumoto et al.

Effects of erythrocyte deformability upon hematocrit assessed by the conductance method
Yoshihito Hayashi, Yoichi Katsumoto, Ikuya Oshige et al.

Study of glucose reaction on erythrocyte membranes
Yoshihito Hayashi, Leonid Livshits, Andreas Caduff et al.

Electrode polarization correction
Yu Feldman, E Polygalov, I Ermolina et al.

Human red blood cells deformed under thermal fluid flow
Ji-Jinn Foo, Vincent Chan, Zhi-Qin Feng et al.

Numerical simulation of dielectric spectra
Antonio di Biasio, Luigi Ambrosone and Cesare Cametti

Time-domain dielectric spectroscopy applied to cell suspensions
S Bone, B Z Ginzburg, H Morgan et al.

Temporal variation of dielectric properties of preserved blood
Yoshihito Hayashi, Ikuya Oshige, Yoichi Katsumoto et al.

IOP Publishing | Institute of Physics and Engineering in Medicine Physiological Measurement

Physiol. Meas. **38** (2017) 1335–1348 https://doi.org/10.1088/1361-6579/aa707a

The dielectric spectroscopy of human red blood cells: the differentiation of old from fresh cells

Marcelo David[1], Evgeniya Levy[1], Yuri Feldman[1], Paul Ben Ishai[1,4,5], Orly Zelig[2], Saul Yedgar[3] and Gregory Barshtein[3]

[1] Applied Physics Department, The Hebrew University of Jerusalem, Jerusalem, Israel
[2] The Hadassah Blood Bank, Hadassah Medical Center, Jerusalem, Israel
[3] Faculty of Medicine, Department of Biochemistry and Molecular Biology, The Hebrew University of Jerusalem, Jerusalem, Israel
[4] Department of Physics, Ariel University, PO Box 3, Ariel 40700, Israel[†]

E-mail: paulbi@ariel.ac.il

Received 28 December 2016, revised 19 April 2017
Accepted for publication 2 May 2017
Published 22 June 2017

Abstract

Objective: The objective of the study was to gauge the effect of storage lesions on the dielectric response of red blood cells (RBC), in particular those processes linked to deformations of the cellular membrane known as the β-dispersion. *Approach*: The dielectric response of RBC suspensions, exposed to blood-bank cold storage, was studied using time-domain dielectric spectroscopy (TDDS) in the frequency range of 500 kHz up to 1 GHz. The measured dielectric processes are characterized by their dielectric strength ($\Delta\varepsilon$) and relaxation time (τ). Changes in the dielectric properties of the RBC suspensions due to storage-related lesions were evaluated. For a quantitative characterization of RBC lesions, we measured the deformability of fresh and stored RBC as expressed by their elongation ratio (ER), which was achieved under a shear stress of 3.0 Pa. *Main Result*: The results show that the storage of RBC induced a statistically significant decrease of dielectric relaxation times. In addition, a sound correlation between the mean values of ER and the relaxation times was observed (Spearman's correlation coefficient $\rho = 0.847$). We draw the conclusion that those alterations in the relaxation time are induced by changes in the shape of the RBC that happen during cold-storage. *Significance*: The evolution of the β-dispersion of RBC opens new possibilities in the blood bank inventory management.

[5] Author to whom any correspondence should be addressed.
[†] Publisher's note: Whilst IOP Publishing adheres to and respects UN resolutions regarding the designations of territories (available at http://www.un.org/press/en), the policy of IOP Publishing is to use the affiliations provided by its authors on its published articles.

 © 2017 Institute of Physics and Engineering in Medicine Printed in the UK

Keywords: dielectric spectroscopy, red blood cells, erythrocytes, aging, storage

(Some figures may appear in colour only in the online journal)

1. Introduction

Donated human red blood cells (RBC) are routinely stored for a period of 35–42 d. This time limit has been determined mainly based on their life span in the circulatory system and on changes in their biochemical parameters (Wolfe 1985). Contrastingly, a growing number of studies have shown that the transfusion of some bank-stored RBC may be a source of injury rather than benefit to the recipients (Sherk *et al* 2000, Glynn 2008, Hillyer *et al* 2008, Leal-Noval *et al* 2008, Almac *et al* 2014). Increased hospital mortality, intubation within 72 h, renal failure, and sepsis or septicaemia are some examples of conditions associated with the use of non-functioning transfused blood (Koch *et al* 2008, Marin *et al* 2013). It was noted that blood storage itself may induce a number of biochemical alterations in RBC properties, such as: an increase in membrane-bound globin (Wolfe *et al* 1986), an oxidation of skeletal proteins, a loss of cellular antioxidant capability (Racek *et al* 1997, Dumaswala *et al* 2000), a decrease in K^+ concentration and subsequent dehydration (Olivieri *et al* 1993), a loss of membrane lipids (Wolfe *et al* 1986, Dumaswala *et al* 2000), a decrease in the cell surface sialic acid (Godin and Caprani 1997), an alteration of the shape of the RBC (Iglic *et al*) and a strong elevation of cell rigidity (decreasing deformability) (Relevy *et al* 2008). Collectively these are known as storage lesions.

Specifically, while fresh and healthy RBC are characterized by a biconcave discoid shape (see figure 1(a)), aged and/or lesioned RBC are typically transformed into echinocytes: i.e. the cells become spheroidal and are sometimes accompanied by the appearance of small thorny projections on their edges (see figure 1(b)) (Hovav *et al* 1999). This shape transformation under cold-storage has been described previously (Iglic *et al*). It may be related to cell vesiculation (Eber *et al* 2001) and/or an alteration of the physical state of the membrane skeleton (Iglic 1997).

RBC vesiculation occurs during cell aging *in vivo* (Yáñez-Mó *et al* 2015) and *in vitro* (Eber *et al* 2001). Differences in the vesicle shedding mechanism *in vivo* and *in vitro* have been described by Bosman *et al* (Bosman *et al* 2008) and Delobel *et al* (Delobel *et al* 2016). However, in both cases vesiculation induced a decrease of the cell-surface-area (Flatt *et al* 2014) by the loss of proteins and lipids from the membrane (Pascual *et al* 1993). Kriebardis *et al* (2007, 2008) demonstrated that the vesicles released during storage of RBCs contain lipid raft proteins and oxidized or reactive signaling components commonly associated with the senescent RBCs.

The alteration of RBC shape is traditionally characterized by electron microscopy. An alternate method to observe morphological changes of the cellular membrane is to study the dielectric response. This was first demonstrated by Höber and others (Höber 1910, 1912, 1913, Fricke 1925, Asami *et al* 1989, Asami 2015) and applied to the aging of Rabbit blood by Hayashi and his team (Hayashi *et al* 2008). They demonstrated that dielectric spectroscopy (DS) is a sensitive tool to monitor deterioration and morphological changes of stored erythrocytes. As these changes in cell morphology lead to differing dielectric interfaces, one would expect Maxwell–Wagner interfacial polarization processes to appear (Asami 2015). These processes are a function of the dielectric properties of each phase (suspension buffer, cell membrane and cytoplasm) and are usually known collectively as the β-dispersion. They are

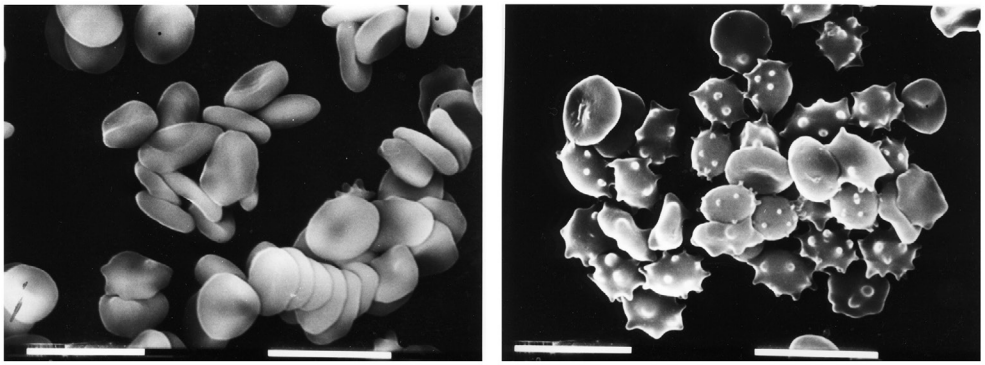

Figure 1. Scanning electron micrographs of RBCs, obtained in our previous research (Hovav *et al* 1999): (a) freshly donated; (b) stored during 35 d.

characterized by a dielectric strength ($\Delta\varepsilon$) and a relaxation time (τ) (Kremer and Schönhals 2003, Asami 2015). In the radio frequency range of MHz, the overall dielectric response of cell suspensions (RBC suspensions in our case) is governed mostly by this phenomenon (Martinsen and Grimnes 2011). Furthermore, the complex dielectric permittivity of a RBC suspension is strongly dependent on the shape of the cells (Sillars 1937, Asami 2015) and it was shown that different shapes of cells affect the overall dielectric spectrum of a suspension (Asami and Yonezawa 1995). In particular, it was shown by Asami *et al* (1980, 1995) that ellipsoid particles in suspension would give rise to two distinct interfacial relaxation processes, whose characteristic relaxation times would be related to the major and minor axes of the ellipsoid respectively. The theory was confirmed by the measurement of human erythrocytes (Asami *et al* 1980).

In this study, we exploit the strength of DS to investigate the alterations (lesion) of human RBC due to cold-storage under standard blood-bank conditions, by studying relative changes in the β-dispersion. In parallel, for an assessment of the level of storage-induced lesions in the cells, we have characterized the deformability of RBC (Relevy *et al* 2008, Barshtein *et al* 2011).

2. Materials and methods

2.1. Study design

Nine samples of fresh RBC (f-RBC) and nine samples of stored RBC (st-RBC) were prepared and then studied simultaneously by means of two different methods: the deformability test (Relevy *et al* 2008) and time-domain dielectric spectroscopy (Feldman *et al* 1992, 1996, Hayashi *et al* 2003).

2.2. Materials

Bovine serum albumin (BSA) was purchased from Amresco (OH, USA), D-Glucose and L-Glucose from Sigma (St. Louis, MO) and un-coated polystyrene slides from Electron Microscopy Science (Washington, PA).

2.3. Collection and preparation of RBC

St-RBC samples were collected from Packed-RBC (PRBC) units (non-leukodepleted, stored in CPDA-1 under 4 °C with a concentration of approximately 60% by volume) after cold-storage of at least 21 d in the blood bank; f-RBC samples were collected directly from healthy donors. Both collections were done with the donor's consent according to the Helsinki Committee Regulations (Permit 98290, Hadassah Hospital, Jerusalem, Israel).

5 ml of st-RBC were drawn from PRBC units. The RBC were then washed three times by centrifugation (500 × g; 7 min) using PBS (Phosphate Buffered Saline), and re-suspended at hematocrit in G-PBS (PBS supplemented with L-Glucose (2.7 mg ml^{-1}) and D-Glucose (0.9 mg ml^{-1})) (Livshits *et al* 2007). Samples of f-RBC were isolated from freshly-donated blood, washed (three time) from their plasma by centrifugation (500 × g; 7 min.) in PBS and re-suspended at hematocrit in G-PBS (Livshits *et al* 2007).

The L-Glucose reduces the electrical conductivity of the buffer (minimizing the effects of electrode polarization (Feldman *et al* 2001, Ben Ishai *et al* 2013) which are discussed in section 2.5.3), and the D-Glucose compensates the osmotic pressure thereby avoiding changes in the cell shape due to the suspension (Livshits *et al* 2007). The measurement took place within 60 min after the washing and the resuspension.

Fresh and stored samples are not related what-so-ever, and were measured on different days, as they were supplied.

2.4. Deformability test

Washed RBC were re-suspended at a hematocrit of 5% in PBS supplemented by 0.5% of bovine albumin. A computerized cell flow-properties analyzer (CFA), designed and constructed in The Hebrew University of Jerusalem (Israel) (Relevy *et al* 2008), was used for testing deformability of the cells. The CFA enables the monitoring of RBC hemodynamic characteristics as a function of shear stress, under conditions that resemble those in microvessels, by direct visualization of their dynamic organization in a narrow-gap flow-chamber, placed under a microscope (Relevy *et al* 2008, Barshtein *et al* 2011). RBC deformability is determined by monitoring the elongation of the cells under flow-induced sheer stress (Relevy *et al* 2008). 50 μl of suspension are inserted into the flow-chamber (adjusted to 200 μm gap) containing an uncoated polystyrene slide. The adherent RBC are then subjected to controllable flow-induced sheer stress (3.0 Pa), and their deformability is determined by the change in cell shape, as expressed by the average elongation ratio: ER = a/b, where a and b are the major and the minor cell axes respectively. ER = 1 reflects a round RBC, non-deformed under the applied sheer stress. The CFA image analysis program measures the ER for each individual cell, provides the deformability distribution in a large RBC population (at least 2500 ± 300 cells) and calculates the average value of ER.

2.5. Time-domain dielectric spectroscopy (TDDS)

For the automated measurement of the dielectric properties of matter, our lab has developed a time-domain dielectric spectrometer based on the Agilent 86100C time-domain reflectometer (Agilent Technologies 2009). Temperature control is provided by a Julabo CF41 heat circulator-thermostat with temperature fluctuations of 0.5 °C. The system is designed for measuring dielectric parameters over the frequency range 100 KHz–20 GHz (the actual upper limit depends on the sample cell's geometry, in this paper it is capped at 1 GHz).

Non-uniform signal sampling (Feldman *et al* 1996, Feldman *et al* 2006) is performed to enhance memory usage, efficiency, and measurement precision. The TDDS's software allows registration, accumulation and collection of data, Fourier analysis (spectra calculation), and time-domain treatment (the latter includes nonlinear curve fitting to extract the dielectric parameters).

2.5.1. Description of the method. The TDDS technique is based on time domain reflectrometry (TDR) (Smith *et al* 2005, Oliver 2016). In TDR a voltage step propagates from the signal generator along the transmission line. Structural discontinuities along the line generate reflected pulses (Pozar 2012, Oliver 2016). As the reflected pulse's shape contains information about the discontinuity, this method can be used to extract dielectric properties of any material placed at any given section of the transmission line (Fellner-Feldegg 1969, Feldman *et al* 1996).

In TDDS, the sample cell (a parallel-plate capacitor) containing the RBC suspension is placed at the end of a 50 Ω transmission line; the reflected signal is superimposed on the incident pulse and the resulting signal (sum of the step voltage and the reflected signal) is recorded at the sampling head. It is then sent to the digital signal processing (DSP) unit (Nozaki and Bose 1990, Feldman *et al* 1996, Berberian and King 2002, Cerný 2009). The system frequency range limits are determined by the pulse rise-time, the duration of the pulse and the sample cell's geometry (see section 2.5.2).

The actual sample response signal is found by writing the total voltage across the sample $V_s(t)$:

$$V_s(t) = V_{in}(t) + V_R(t) \tag{1}$$

While the total current through the simple is given by:

$$I(t) = \frac{1}{Z_0} \cdot [V_{in}(t) - V_R(t)] \tag{2}$$

Where $V_{in}(t)$ is the incident voltage, $V_R(t)$ is the reflected signal, and Z_0 is the characteristic line impedance (Feldman *et al* 1992). Using a lumped-capacitance approximation, the governing equation in the time-domain is given by:

$$Q(t) = C_c \cdot \left[\varepsilon_\infty \cdot V_s(t) + (\varepsilon_s - \varepsilon_\infty) \cdot \int_0^t \frac{d\phi(t-t')}{dt} \cdot V_s(t')\, dt'\right] \tag{3}$$

Where $Q(t)$ is the total charge in the capacitor, $\phi(t)$ is the dielectric response function of the sample, C_c is the vacuum capacitance of the sample cell, ε_s and ε_∞ are the static and high-frequency dielectric constants, respectively. $Q(t)$ can be calculated by simple integration in the time of the current signal $I(t)$ obtained by equation (2).

After applying the Fourier Transform to equation (3), the charge can be expressed as (Böttcher *et al* 1980, Martinsen and Grimnes 2011):

$$Q(\omega) = C_c \cdot \varepsilon(\omega) \cdot V_s(\omega) \tag{4}$$

Where the complex permittivity is the Fourier image of the derivative of the dielectric step-response function:

$$\varepsilon(\omega) = \varepsilon_\infty + (\varepsilon_s - \varepsilon_\infty) \cdot \int_0^\infty \frac{d\phi(t)}{dt} \cdot e^{-j\omega t} dt = \varepsilon_\infty + (\varepsilon_s - \varepsilon_\infty) \cdot F\left\{\frac{d\phi(t)}{dt}\right\} \tag{5}$$

Figure 2. Teflon ring sitting on bottom electrode and holding a drop of RBC suspension.

In order to extract the dielectric properties of the material-under-test, the dielectric response function should be fitted to a previously known descriptive function, after it has been obtained by deconvolution of equation (3). In the case of a pure Debye process, the dielectric response can be fitted to equation (6):

$$\phi(t) = \left[\varepsilon_\infty + \Delta\varepsilon \cdot \left(1 - \mathrm{e}^{-\frac{t}{\tau}}\right)\right] \quad t \geqslant 0 \tag{6}$$

2.5.2. Sample cell. A capacitor of parallel plates terminates the coaxial transmission line. There is a need to maintain the same line impedance, regardless of the plate diameter, otherwise spurious reflections are generated. This was achieved by inserting a series of coaxial steps between the plate capacitor and the coaxial line, such that each step maintains the same characteristic line impedance.

For MHz frequencies, coaxial transmission-line segments have a characteristic impedance that can be approximated by:

$$Z_i = \frac{1}{2\pi} \cdot \sqrt{\frac{\mu}{\varepsilon}} \cdot \ln\left(\frac{d_{\mathrm{out}}}{d_{\mathrm{in}}}\right) \tag{7}$$

Where ε, μ, d_{out} and d_{in} are the permittivity, the permeability and the outer and inner radii of the transmission line's dielectric, respectively (Staniforth 2016).

The highest usable frequency of the coaxial line is given by:

$$f_{\max} = \frac{c \cdot k_{\mathrm{c}}}{2\pi \cdot \sqrt{\varepsilon_{\mathrm{r}}}} \tag{8}$$

Where c is the speed of light, ε_{r} is the relative permittivity of the transmission line's dielectric, and $k_{\mathrm{c}} = \frac{4}{d_{\mathrm{in}}+d_{\mathrm{out}}}$ (Pozar 2012). In this study, the sample cell has $d_{\mathrm{in}} = 24\,\mathrm{mm}$ and $d_{\mathrm{out}} = 60\,\mathrm{mm}$, and air is the line's dielectric, giving a maximum working frequency of about $f_{\max} = 2.3$ GHz.

Since the electrodes need to be made of a biocompatible material, we chose to use polished 316L Stainless steel. In order to hold the RBC suspension between the electrodes, a Teflon ring was used as shown in figure 2. The Teflon ring fits tight over the bottom electrode and has an aperture in its center of 5 mm of diameter; the height of the ring is 1.75 mm. Therefore, a volume of 34 μl is held.

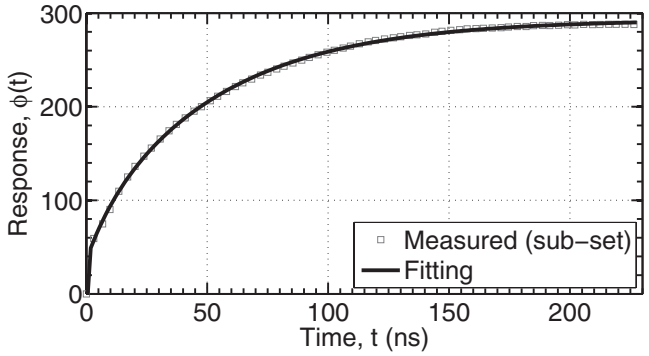

Figure 3. The dielectric step response function for sample F1: measured and fitted.

2.5.3. Electrode polarization. Typically, when performing dielectric spectroscopy of conducting systems which contain dissolved free ions (e.g. colloids and cell suspensions), a phenomenon called electrode polarization (EP) occurs: when applying an electric field, dissolved free ions tend to move towards and accumulate on the electrode-suspension interfaces. The electric potential drops significantly in the polarization layers, leading to a strong polarization of those layers and, in the worst case, an almost absence of the electric field in the actual suspension. Several techniques were proposed to correct the effect of Electrode Polarization and obtain the bulk sample dielectric response function (Feldman *et al* 1998, 2001, Ben Ishai *et al* 2013). The parallel-plate geometry of the sample cell in our study leads to the assumption that the EP layers are similar and parallel on both electrodes. Therefore, in this case, the response due to electrode polarization can be modeled in the time domain according to the so-called single exponent approximation (Feldman *et al* 2001, Ben Ishai *et al* 2013). In TDDS this approximation proposes that EP adds a parasitic signal to the sample's step response function (Feldman *et al* 1992, Ben Ishai *et al* 2013), which can be fitted to equation (9):

$$V_{\mathrm{ep}}(t) = A_0 \left(1 - \mathrm{e}^{-\frac{t}{\tau_{\mathrm{EP}}}}\right) \tag{9}$$

It is important to note that EP governs the response signal at low frequencies: i.e. the parasitic signal is time delayed from the sample's step response function, making it easy to fit equation (9), and to correct the acquired signal. The software of our TDDS system performs the corresponding correction.

2.6. DS measurements of RBC suspensions

For each one of the RBC samples (fresh and stored), the following procedure was performed: the parallel-plate sample cell was filled with 35 μl of the prepared suspension (see section 2.3), and then stabilized at 25 °C using the temperature control module. The sample was measured 16 times; after averaging the measurements, the resulting signal was digitally processed as described above.

3. Results and discussion

Nine samples of f-RBC and nine of st-RBC were measured by means of TDDS. To fit the results it was necessary to employ two Debye processes. The fitting function is presented in equation (10):

Table 1. Average dielectric parameters of fresh and stored RBC.

	$\Delta\varepsilon_1$	τ_1	$\Delta\varepsilon_2$	τ_2	ε_∞
Fresh RBC	188.9	59.53	44.2	10.73	65.7
Stored RBC	176.0	44.28	32.4	0.42	64.2

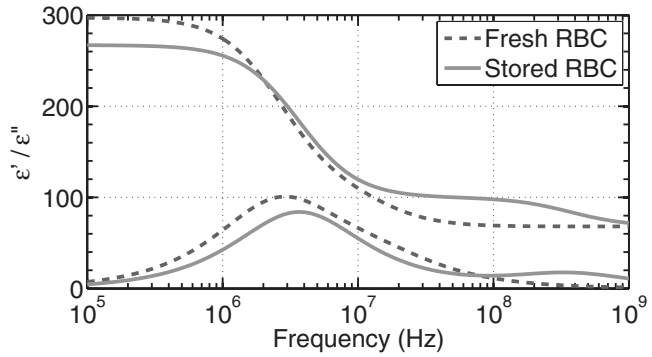

Figure 4. The reconstructed dielectric spectra, based on the averaged fitting parameters of all Fresh and all Stored RBC suspensions.

$$\phi(t) = \left[\varepsilon_\infty + \Delta\varepsilon_1 \cdot \left(1 - \mathrm{e}^{-\frac{t}{\tau_1}}\right) + \Delta\varepsilon_2 \cdot \left(1 - \mathrm{e}^{-\frac{t}{\tau_2}}\right)\right] \quad t \geqslant 0 \tag{10}$$

Where ε_∞ is the high frequency limit of the permittivity of the suspension, and $\Delta\varepsilon_i$ and τ_i are the dielectric strength and the time constant of the process *i*, respectively. In figure 3 we present an example case (namely sample F1—see table 3) of the measured dielectric response function after performing EP correction (Feldman *et al* 2001, Ben Ishai *et al* 2013), and its fitting to equation (10). In table 1 we present the average dielectric parameters values obtained for all fresh and all stored RBC suspensions; in figure 4 the calculated average dielectric spectra for both cases are shown.

Due to the characteristic biconcave shape of normal erythrocytes (see figure 1(a)), one would expect to see two main dielectric processes: one process corresponds to the external radius of the discocyte while the second process corresponds to the cell width. Both processes should be considered to be pure Debye, as expected for Maxwell–Wagner polarization processes, as noted in equation (10).

Upon aging of the RBCs it was still necessary to use equation (10) to fit the data. The implication is that there are still two length scales involved, despite the expectation that the erythrocytes would have become echinocyte-shaped (with reduced cell radius) (Mohandas and Chasis 1993, Barshtein *et al* 2011, 2014). This new shape, as discussed above, is characterized by the spheroid radius of the echinocyte, but may also be influenced by thorny projections that are sometimes observed (see figure 1(b)). Furthermore, the fast process, τ_2, is significantly shifted towards the higher frequencies, indicating much smaller length scales than those of the minor RBC axis. An obvious candidate in this case could be the appearance of these same thorny projections (see figure 1(b)) of the stored RBC.

It is relatively simple to explain the increase in τ_1: in the case of fresh erythrocytes (biconcave discoid), τ_1 is related to the disc radius while τ_2 is related to the cell width. For larger sizes of particles one would expect to obtain longer relaxation times (Sillars 1937, Looyenga 1965, Asami *et al* 1980, Stroud 1998, Asami 2002). The external radius of the RBC decreases

Table 2. t-student tests for fresh and stored RBC suspensions.

	Fresh RBC		Stored RBC			
	Average	Variance	Average	Variance	t-stat	t-critical (two tails)
τ_1	59.53	5.36	44.28	24.24	8.39	2.31 $p = 3.07 \times 10^{-5}$
τ_2	10.73	0.57	0.42	0.02	34.28	2.45 $p = 1.79 \times 10^{-11}$
ER	1.78	3.55×10^{-3}	1.53	0.02	4.31	2.31 $p = 2.57 \times 10^{-3}$

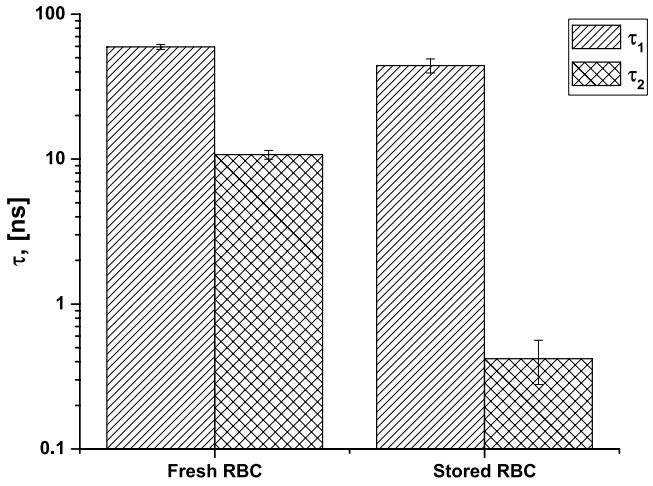

Figure 5. Average characteristic relaxation times of Fresh and Stored RBC suspensions for nine RBC samples, obtained from freshly donated blood and stored units. $*p = 3.07 \times 10^{-5}$ $**p = 1.79 \times 10^{-11}$ for a non-pair t-test.

with storage time (Jaferzadeh and Moon 2015) and so, we would expect τ_1 of the fresh erythrocytes to be greater than that of the stored ones. The width of normal erythrocytes is within the order of magnitude of the main disc radius of both fresh and stored erythrocytes and, therefore, we see that τ_2 is within the order of magnitude of τ_1 of both fresh and stored erythrocytes.

It is well documented that the alteration of RBC shape under cold storage (Hovav *et al* 1999) is often accompanied by a decrease in RBC's deformability (Berezina *et al* 2002, Relevy *et al* 2008, Barshtein *et al* 2011, 2014). In addition, the role of the cell's shape in RBC deformability has been previously noted by Mohandas and Chasis (1993). Thus Izzo *et al* (1999) demonstrated that erythrocyte deformability is impaired by membrane and cytoskeleton structure anomalies and by changes in the red cell area/volume ratio. In tables 3(a) and (b) we present the ER (deformability test) and the TDDS fitting values for the fresh and stored samples, respectively. Figure 4 shows the reconstructed spectra, based on the averaged values of the relaxation times τ_1 and τ_2 of f-RBC and st-RBC suspensions; t-Student tests were performed in order to test the hypothesis that f-RBC and st-RBC can be classified using the dielectric relaxation times. Table 2 shows the results of the tests. The t-tests show that the null hypotheses can be discarded; thus, both distributions (f-RBC and st-RBC) can be considered to be different. The results are represented graphically in figure 5. Note that in order to perform a Student's t-test, the data should be normally distributed. All the samples were randomly chosen from the blood bank, each from different donors. As a result, we performed an Anderson–Darling test for a normal distribution of the data points (Anderson and Darling

Table 3. Average and standard deviation of ER and Fitting values of human RBC samples. *P*-value refers to the Anderson–Darling test for normal distribution *P* values. $P > 0.05$ implies that the samples are normaly distributed.

3(a)—(Fresh human RBC samples)						
Sample #	ER	$\Delta\varepsilon_1$	τ_1	$\Delta\varepsilon_2$	τ_2	ε_∞
F1	1.87 ± 0.04	171.27 ± 7.71	59.67 ± 5.48	44.31 ± 1.16	11.34 ± 0.54	62.09 ± 2.62
F2	1.70 ± 0.05	204.87 ± 9.19	58.52 ± 1.49	42.78 ± 4.04	10.20 ± 0.97	65.50 ± 2.04
F3	1.80 ± 0.04	188.67 ± 8.40	62.11 ± 1.49	43.20 ± 3.71	11.62 ± 1.02	68.21 ± 1.83
F4	1.80 ± 0.05	174.73 ± 4.76	56.01 ± 2.30	42.65 ± 2.33	10.42 ± 0.59	67.12 ± 1.75
F5	1.70 ± 0.04	174.55 ± 15.14	60.52 ± 0.28	48.10 ± 7.11	11.72 ± 0.54	64.72 ± 4.78
F6	1.77 ± 0.03	158.92 ± 8.39	55.96 ± 9.36	40.38 ± 15.88	9.41 ± 3.83	68.60 ± 6.28
F7	1.80 ± 0.05	209.46 ± 19.05	61.55 ± 3.21	46.71 ± 21.32	10.95 ± 1.64	67.93 ± 8.10
F8	1.84 ± 0.04	227.46 ± 9.60	59.68 ± 0.46	42.45 ± 1.16	10.26 ± 0.14	65.26 ± 8.08
F9	1.74 ± 0.03	190.25 ± 8.36	61.75 ± 2.11	47.23 ± 5.19	10.69 ± 1.20	62.09 ± 4.01
P-value	0.529	0.683	0.253	0.289	0.828	0.341
3(b)—(Stored human RBC samples. S4 and S9 could only be fitted using one Debye process)						
Sample #	ER	$\Delta\varepsilon_1$	τ_1	$\Delta\varepsilon_2$	τ_2	ε_∞
S1	1.35 ± 0.04	152.74 ± 0.07	35.80 ± 1.87	33.95 ± 1.61	0.36 ± 0.03	62.20 ± 1.56
S2	1.36 ± 0.03	166.05 ± 15.96	43.45 ± 3.64	39.86 ± 9.58	0.40 ± 0.10	68.63 ± 5.50
S3	1.38 ± 0.05	142.64 ± 6.76	38.79 ± 0.67	35.63 ± 3.92	0.31 ± 0.03	59.33 ± 2.60
S4	1.49 ± 0.04	146.33 ± 18.10	41.02 ± 0.62	—	—	60.59 ± 4.34
S5	1.70 ± 0.03	186.75 ± 2.40	50.72 ± 0.08	37.70 ± 0.17	0.72 ± 0.02	64.93 ± 1.91
S6	1.53 ± 0.05	192.62 ± 16.25	48.15 ± 2.02	22.96 ± 1.80	0.41 ± 0.09	64.58 ± 4.56
S7	1.69 ± 0.04	184.15 ± 10.18	45.22 ± 1.03	20.51 ± 1.11	0.37 ± 0.04	68.37 ± 5.21
S8	1.68 ± 0.04	137.40 ± 10.49	47.72 ± 0.97	36.32 ± 0.21	0.39 ± 0.01	65.26 ± 2.24
S9	1.61 ± 0.03	275.20 ± 14.62	47.66 ± 2.03	—	—	64.20 ± 6.10
P-value	0.217	0.056	0.574	0.065	0.003	0.626

1952). The results are presented in tables 3(a) and (b) along with the ER and the TDDS fitting values. A *P*-value greater than 0.05 indicates that the data is normally distributed. This condition is fulfilled by the majority of the data, except for the relaxation times, τ_2, of the second process in stored RBC. In this case the dielectric strength manages to pass the test while the relaxation times are borderline. However, due to biological variance and since the median and average values of the measurements are almost equal (relative difference of 0.5%), we conclude that the measurements are indeed normally distributed.

Figure 6 shows a strong correlation between ER and τ_1 and between ER and τ_2. The correlation values were calculated using Spearman's ranked correlation coefficient. While τ_1 shows an almost linear correlation to ER, both parameters demonstrate a marked differentiation between the populations of fresh and stored RBC. This is particularly clear for τ_2 and may point to the emergence of a new source for the relaxation. An obvious candidate would be the formation of the thorny nodules, noted in figure 1(b). The observed correlation between τ_1 and ER can be related to the fact that both of these parameters are modulated by the cells' shapes, which are altered under cold-storage (Hovav *et al* 1999). It should be noted that in their 2008 paper Hayashi *et al* used a single Cole-Cole relaxation model for fitting their measurements. While Hayashi *et al* saw an increment in the relaxation time of the Cole–Cole process, we see

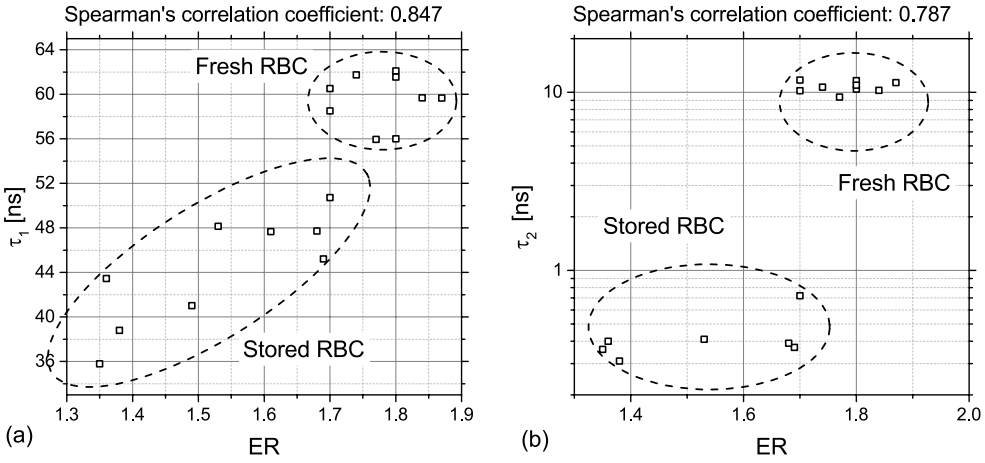

Figure 6. (a) τ_1 and (b) τ_2 plotted against Elongation ratio (ER). The Spearman ranked correlation coefficients are 0.847 and 0.787 respectively, indicating a strong correlation of the β dispersion on cell shape.

a decrement of both Debye's relaxation times. Hayashi *et al* explained the increment in the Cole–Cole relaxation time as a consequence of changes in the cytoplasm's conductivity of the studied cells during aging. It is important to note that in Hayashi *et al*'s experiment rabbit cells were used and, in addition, cell storage conditions strongly differ from the storage and preparation protocol used in our study (Hayashi *et al* 2008).

Based on our results we can suggest the following scheme. It is well documented that the cold-storage accelerates a number of parallel processes in RBC: specifically, membrane vesiculation (that induces loss of membrane area) and reorganization of cytoskeleton. Both of these alterations lead to cellular shape transformation (from discoid to spherical) and decrease the deformability. In parallel, we observed a drastic difference in DS of freshly donated cells and erythrocytes that have been stored during 35 d in blood bank.

4. Conclusions

By means of dielectric spectroscopy (DS) we have analyzed the β-dispersion dielectric spectra of both freshly donated and stored RBC suspensions, in order to determine whether DS are sensitive to the alteration of RBC that caused by long (of at least 21 d) cold-storage. The data were modeled on the basis of two pure Debye processes: in the case of fresh (healthy) RBC, one process corresponds to the discoid radius and the second process corresponds to the cell width; in the case of stored (lesioned) RBC, one process corresponds to the spheroid radius and the second process may correspond to the small thorny projections of the cell. The obtained results show that a cold-storage of erythrocytes induces a marked elevation of the value of first relaxation time (τ_1) and these alterations can be related to cells lesion. Furthermore, we observed a strong correlation between τ_1 and the mean Elongation Ratio of the RBC population under shear stress of 3.0 Pa. These findings suggest that the relaxation times of RBC suspensions (by means of DS in the MHz frequency range) are very sensitive to long cold-storage.

Acknowledgments

This study was supported by a grant from the Israel Science Foundation (to P Ben Ishai and G Barshtein; 1661/13). We thank Ms Olga Fredman (The Hebrew University of Jerusalem, Faculty of Medicine) and Hanna Greenbaum (Blood Bank, Hadassah University Hospital) for their technical assistance. The Authors would like to thank Prof R Glaser and Mr Kevin Otto for the use of their Anderson–Darling Normality Test Calculator spreadsheet.

References

Almac E, Bezemer R, Hilarius-Stokman P M, Goedhart P, de Korte D, Verhoeven A J and Ince C 2014 Red blood cell storage increases hypoxia-induced nitric oxide bioavailability and methemoglobin formation *in vitro* and *in vivo Transfusion* **54** 3178–85

Anderson T W and Darling D A 1952 Asymptotic theory of certain 'goodness of fit' criteria based on stochastic processes *Ann. Math. Stat.* **23** 193–212

Asami K 2002 Characterization of heterogeneous systems by dielectric spectroscopy *Prog. Polym. Sci.* **27** 1617–59

Asami K 2015 Radiofrequency dielectric properties of cell suspensions *Dielectric Relaxation in Biological Systems: Physical Principles, Methods, and Application* ed Y Feldman and V Raicu (Oxford: Oxford University Press)

Asami K and Yonezawa T 1995 Dielectric behavior of non-spherical cells in culture *Biochim. Biophys. Acta* **1245** 317–24

Asami K, Hanai T and Koizumi N 1980 Dielectric approach to suspensions of ellipsoidal particles covered with a shell in particular reference to biological cells *Japan. J. Appl. Phys.* **19** 359–65

Asami K, Takahashi Y and Takashima S 1989 Dielectric properties of mouse lymphocytes and erythrocytes *Biochim. Biophys. Acta* **1010** 49–55

Barshtein G, Gural A, Manny N, Zelig O, Yedgar S and Arbell D 2014 Storage-induced damage to red blood cell mechanical properties can be only partially reversed by rejuvenation *Transfus. Med. Hemotherapy* **41** 1

Barshtein G, Manny N and Yedgar S 2011 Circulatory risk in the transfusion of red blood cells with impaired flow properties induced by storage *Transfus. Med. Rev.* **25** 24–35

Ben Ishai P, Talary M S, Caduff A, Levy E and Feldman Y 2013 Electrode polarization in dielectric measurements: a review *Meas. Sci. Technol.* **24** 102001

Berberian J G and King E 2002 An overview of time domain spectroscopy *J. Non-Cryst. Solids* **305** 10–18

Berezina T L, Zaets S B, Morgan C, Spillert C R, Kamiyama M, Spolarics Z, Deitch E A and Machiedo G W 2002 Influence of storage on red blood cell rheological properties *J. Surg. Res.* **102** 6–12

Bosman G J C G M, Werre J M, Willekens F L A and Novotný V M J 2008 Erythrocyte ageing *in vivo* and *in vitro*: structural aspects and implications for transfusion *Transfus. Med.* **18** 335–47

Böttcher C J F and Bordewijk P 1980 *Theory of Electric Polarization: Dielectrics in Time-Dependent Fields* vol II (Amsterdam: Elsevier) p 561 (*Ber. Bunsenges. Phys. Chem.* **84** 1190–1)

Cerný R 2009 Time-domain reflectometry method and its application for measuring moisture content in porous materials: a review *Measurement* **42** 329–36

Delobel J, Barelli S, Canellini G, Prudent M, Lion N and Tissot J-D 2016 Red blood cell microvesicles: a storage lesion or a possible salvage mechanism *ISBT Sci. Ser.* **11** 171–7

Dumaswala U J, Wilson M J, Wu Y L, Wykle J, Zhuo L, Douglass L M and Daleke D L 2000 Glutathione loading prevents free radical injury in red blood cells after storage *Free Radical Res.* **33** 517–29

Eber B I S, Hägerstrand H, Iglic A, Bobrowska-Hägerstrand M and Lindqvist C 2001 Amphiphile-induced vesiculation in aged hereditary spherocytosis erythrocytes indicates normal membrane stability properties under non-starving conditions *Mol. Membr. Biol.* **18** 221–7

Feldman Y D, Zuev Y F, Polygalov E A and Fedotov V D 1992 Time domain dielectric spectroscopy. A new effective tool for physical chemistry investigation *Colloid Polym. Sci.* **270** 768–80

Feldman Y, Andrianov A, Polygalov E, Ermolina I, Romanychev G, Zuev Y and Milgotin B 1996 Time domain dielectric spectroscopy: an advanced measuring system *Rev. Sci. Instrum.* **67** 3208–16

Feldman Y, Nigmatullin R, Polygalov E and Texter J 1998 Fractal-polarization correction in time domain dielectric spectroscopy *Phys. Rev.* E **58** 7561–5
Feldman Y, Polygalov E, Ermolina I, Polevaya Y and Tsentsiper B 2001 Electrode polarization correction in time domain dielectric spectroscopy *Meas. Sci. Technol.* **12** 1355
Feldman Y, Puzenko A and Ryabov Y 2006 Dielectric relaxation phenomena in complex systems *Fractals Diffusion Relaxation Disorder Complex System Part A* ed Y Kalmykov and W Coffey (Hoboken, NJ: Wiley)
Fellner-Feldegg H 1969 Measurement of dielectrics in the time domain *J. Phys. Chem.* **73** 616–23
Flatt J F, Bawazir W M and Bruce L J 2014 The involvement of cation leaks in the storage lesion of red blood cells *Front. Physiol.* **5** 214
Fricke H 1925 The electric capacity of suspensions with special reference to blood *J. Gen. Physiol.* **9** 137–52
Glynn S A 2008 Blood supply safety: an NHLBI perspective *Transfusion* **48** 1541–4
Godin C and Caprani A 1997 Effect of blood storage on erythrocyte/wall interactions: implications for surface charge and rigidity *Eur. Biophys. J.* **26** 175–82
Hayashi Y, Livshits L, Caduff A and Feldman Y 2003 Dielectric spectroscopy study of specific glucose influence on human erythrocyte membranes *J. Phys. Appl. Phys.* **36** 369
Hayashi Y, Oshige I, Katsumoto Y, Omori S, Yasuda A and Asami K 2008 Temporal variation of dielectric properties of preserved blood *Phys. Med. Biol.* **53** 295
Hillyer C D, Blumberg N, Glynn S A, Ness P M and For the Members of the NHLBI Working Group in Transfusion Recipient Epidemiology and Outcomes Research 2008 Transfusion recipient epidemiology and outcomes research: possibilities for the future *Transfusion* **48** 1530–7
Höber R 1910 Eine Methode, die elektrische Leitfähigkeit im Innern von Zellen zu messen *Pflüg. Arch. Gesamte Physiol. Menschen Tiere* **133** 237–53
Höber R 1912 Ein zweites Verfahren, die Leitfähigkeit im Innern von Zellen zu messen *Pflüg. Arch. Gesamte Physiol. Menschen Tiere* **148** 189–221
Höber R 1913 Messungen der inneren Leitfähigkeit von Zellen *Pflüg. Arch. Gesamte Physiol. Menschen Tiere.* **150** 15–45
Hovav T, Yedgar S, Manny N and Barshtein G 1999 Alteration of red cell aggregability and shape during blood storage *Transfusion* **39** 277–81
Iglic A 1997 A possible mechanism determining the stability of spiculated red blood cells *J. Biomech.* **30** 35–40
Iglic A, Kralj-Iglic V and Hägerstrand H Amphiphile induced echinocyte-spheroechinocyte transformation of red blood cell shape *Eur. Biophys. J.* **27** 335–9
Izzo P, Manicone A, Spagnuolo A, Lauta V M, Di Pasquale A and Di Monte D 1999 Erythrocytes stored in CPD SAG-mannitol: evaluation of their deformability *Clin. Hemorheol. Microcirc.* **21** 335–9
Jaferzadeh K and Moon I 2015 Quantitative investigation of red blood cell three-dimensional geometric and chemical changes in the storage lesion using digital holographic microscopy *J. Biomed. Opt.* **20** 111218
Keysight Technologies 2009 86100C Infiniium DCA-J Wide-Bandwidth Oscilloscope Quick Start Guide http://literature.cdn.keysight.com/litweb/pdf/86100-90117.pdf (Accessed: 11 May 2017))
Koch C G, Li L, Sessler D I, Figueroa P, Hoeltge G A, Mihaljevic T and Blackstone E H 2008 Duration of red-cell storage and complications after cardiac surgery *New Engl. J. Med.* **358** 1229–39
Kremer F and Schönhals A (ed) 2003 *Broadband Dielectric Spectroscopy* (Berlin: Springer)
Kriebardis A G, Antonelou M H, Stamoulis K E, Economou-Petersen E, Margaritis L H and Papassideri I S 2007 Storage-dependent remodeling of the red blood cell membrane is associated with increased immunoglobulin G binding, lipid raft rearrangement, and caspase activation *Transfusion* **47** 1212–20
Kriebardis A G, Antonelou M H, Stamoulis K E, Economou-Petersen E, Margaritis L H and Papassideri I S 2008 RBC-derived vesicles during storage: ultrastructure, protein composition, oxidation, and signaling components *Transfusion* **48** 1943–53
Leal-Noval S R, Munoz-Gomez M P, Arellano-Orden V, Marin-Caballos A, Amaya-Villar R, Marin A, Puppo-Moreno A, Ferrandiz-Millon C, Flores-Cordero J M and Murillo-Cabezas F 2008 Impact of age of transfused blood on cerebral oxygenation in male patients with severe traumatic brain injury *Crit. Care Med.* **36** 1290–6
Livshits L, Caduff A, Talary M S and Feldman Y 2007 Dielectric response of biconcave erythrocyte membranes to D- and L-glucose *J. Phys. Appl. Phys.* **40** 15

Looyenga H 1965 Dielectric constants of heterogeneous mixtures *Physica* **31** 401–6
Marin T, Moore J, Kosmetatos N, Roback J D, Weiss P, Higgins M, McCauley L, Strickland O L and Josephson C D 2013 Red blood cell transfusion–related necrotizing enterocolitis in very-low-birthweight infants: a near-infrared spectroscopy investigation *Transfusion* **53** 2650–8
Martinsen O G and Grimnes S 2011 *Bioimpedance and Bioelectricity Basics* (New York: Academic)
Mohandas N and Chasis J 1993 Red blood cell deformability, membrane material properties and shape: regulation by transmembrane, skeletal and cytosolic proteins and lipids *Semin. Hematol.* **30** 171–92
Nozaki R and Bose T K 1990 Broadband complex permittivity measurements by time-domain spectroscopy *IEEE Trans. Instrum. Meas.* **39** 945–51
Oliver B M 2016 Square wave and pulse testing of linear systems *Hewlett Packard Application Note 17, 166* (Colorado Springs, CO: Hewlett Packard) http://bee.mif.pg.gda.pl/ciasteczkowypotwor/HP/Publikacje/an_17.pdf (Accessed: 11 July 2016)
Olivieri O, de Franceschi L, de Gironcoli M, Girelli D and Corrocher R 1993 Potassium loss and cellular dehydration of stored erythrocytes following incubation in autologous plasma: role of the KCI cotransport system *Vox Sang.* **65** 95–102
Pascual M, Lutz H U, Steiger G, Stammler P and Schifferli J A 1993 Release of vesicles enriched in complement receptor 1 from human erythrocytes *J. Immunol.* **151** 397–404 (PMID: 8326133)
Pozar D 2012 *Microwave Engineering* 4th edn (Hoboken, NJ: Wiley)
Racek J, Herynková R, Holecek V, Jerábek Z and Sláma V 1997 Influence of antioxidants on the quality of stored blood *Vox Sang.* **72** 16–9
Relevy H, Koshkaryev A, Manny N, Yedgar S and Barshtein G 2008 Blood banking-induced alteration of red blood cell flow properties *Transfusion* **48** 136–46
Sherk P A, Granton J T and Kapral M K 2000 Red blood cell transfusion in the intensive care unit *Intensive Care Med.* **26** 344–6
Sillars R W 1937 The properties of a dielectric containing semiconducting particles of various shapes *Inst. Electr. Eng.-Proc. Wirel. Sect. Inst.* **12** 139–55
Smith P, Furse C and Gunther J 2005 Analysis of spread spectrum time domain reflectometry for wire fault location *IEEE Sens. J.* **5** 1469–78
Staniforth J A 2016 *Microwave Transmission* (London: The English Universities Press)
Stroud D 1998 The effective medium approximations: some recent developments *Superlattices Microstruct.* **23** 567–73
Wolfe L C 1985 The membrane and the lesions of storage in preserved red cells *Transfusion* **25** 185–203
Wolfe L C, Byrne A M and Lux S E 1986 Molecular defect in the membrane skeleton of blood bank-stored red cells. Abnormal spectrin-protein 4.1-actin complex formation *J. Clin. Invest.* **78** 1681–6
Yáñez-Mó M *et al* 2015 Biological properties of extracellular vesicles and their physiological functions *J. Extracell. Vesicles* **4** 27066–125